ASHESI UNIVERSITY COLLEGE

Fabrication of 3D Printed Scaffolds for Tissue Engineering: Understanding the Mechanical Stability, Degradation Mechanisms and Biocompatibility.

CAPSTONE PROJECT

B.Sc. Mechanical Engineering

Melvin Quashie

(ID: 29592019)

2019

ASHESI UNIVERSITY COLLEGE

Fabrication of 3D Printed Scaffolds for Tissue Engineering: Understanding the Mechanical Stability Degradation Mechanisms and Biocompatibility.

CAPSTONE PROJECT

Capstone Project submitted to the Department of Engineering, Ashesi University in partial fulfilment of the requirements for the award of Bachelor of Science degree in Mechanical Engineering.

Melvin Quashie

(ID: 29592019)

2019

DECLARATION

I hereby declare that this capstone is the result of my own original work and that no part of it has been presented for any other degree in this University or elsewhere.

Candidate's Signature:

……

Candidate's Name:

……

Date:

……

I hereby declare that preparation and presentation of this capstone were supervised in accordance with the guidelines on supervision of capstone laid down by Ashesi University.

Supervisor's Signature:

……

Supervisor's Name:

……

Date:

……

Acknowledgements

This project would not have been possible without the support and contribution of several individuals. Firstly, I am grateful to God for the patience, knowledge and resilience needed to complete this project. I would also like to thank my supervisor Dr. Danyuo Yiporo for his guidance and constant feedback which helped me throughout the progression of this project.

Secondly, I would like to thank Joseph Timpabi and Nicholas Korblah Tali for the procurement of the materials necessary for the completion of this project. I would like to also thank my family and friends who constantly helped me find answers to every question and shared their own ideas on the problems faced throughout the project.

Finally, I would like to thank all the lecturers I have had the honour of studying under through my stay at Ashesi.

Abstract

Diabetes mellitus, also known as diabetes has on major effect on its patients. This is the effect of impaired wound healing. Patients thus get minor wounds such as small cuts which become non-healing and are liable to get infected. Severe cases of such occasions lead to amputations. A solution to this problem is tissue regeneration with the help of scaffolds. These scaffolds are made of biopolymers and promote cell adhesion, regeneration and minimal diffusional constraints.

Computer Aided Design (CAD) software (SolidWorks), was used to design models of scaffolds. Three dimensional (3D) scaffolds were then 3D printed. Scaffolds were also casted using PLA and a mixture of PLA and PEG. The models along with its samples undergo tensile, stiffness and mass degradation tests to gain insight on whether this model is applicable.

Computer simulations were used to evaluate the tensile properties under real world conditions. Furthermore, a universal testing machine was then used to validate the properties obtained from the computer simulations. There was no significant difference in the methods. Optical properties were characterised with USB poroscope imaging microscope to show that 3D printing produces much more uniform distribution of pores. Mass loss experiments were also conducted to determine mechanical stability at different pH. It was noticed that the samples degrade faster when in an acidic environment.

Table of Contents

List of Figures

List of Tables

Chapter One

1.0 Introduction

1.1 Introduction and Background Studies

Scaffolds play major roles in tissue engineering, especially in the field of tissue regeneration. Organ or tissue loss or failure due to injuries or other means is a major problem in the surgical fields of medicine [1,18]. Transplantation of viable organs or tissue has been the standard method of treating patients [1,18]. Unfortunately, this method has some shortcomings as donors with viable tissue are limited. Moreover, tissue grafting, and alloplastic or synthetic material replacement are also commonly known methods of tissue repair [1]. However, these approaches also have limitations. For example, tissue grafting requires second surgical sites with related injury and is constrained by limited amounts of material to be used as synthetic materials. Most often, grafted tissue/organ integrate poorly with host tissue and fail over time due to wear and fatigue and can show signs of rejection with the patient's body [1].

Tissue engineering is an alternative and promising method of treating tissue related ailments. This method was developed in the early1990s to address shortcomings of tissue grafting and alloplastic tissue repair [1]. This method involves the transplant and culturing of bio factors (cells, genes and/or proteins) within a degradable porous structure known as a scaffold [1,18]. The culturing of these cells forms the new organ or tissue, and this is usually done with the patient's cells.

The design and fabrication of these scaffolds can be achieved using various methods. Some methods include solvent casting [2], electro spinning [2], phase separation technique [2] and solid free form fabrication [2]. Computer aided design (CAD) techniques has been used to print scaffolds, layer by layer [3]. This is done by depositing the base material of the

scaffolds to form a three-dimensional (3D) structure. Scaffolds need to have specific mechanical properties to perform in a way that they are intended to. Properties of the scaffold such as porosity and degradation mechanism also affect the performance of the scaffolds.

Functional scaffolds are usually made of biopolymers (with large molecular weight) with well- defined pore-microstructures, specific surface area and chemical composition to promote cell adhesion, regeneration and minimal diffusional constraints [9]. Moreover, the scaffold must also have good mechanical and structural properties, be biocompatible and biodegradable and be able to undergo sterilization without loss of properties. [2].

Scaffold fabrication using 3D printing is a relatively new method of fabrication. Scaffolds design and fabrication with 3D printers would be explored for the effect of manufacturing processes on the mechanical properties of a scaffold coupled with adequate based material properties of scaffolds for the development of soft tissue such as skin.

1.2 Problem Definition

Diabetes mellitus, usually referred to as diabetes, is a group of metabolic disorders in which there are high blood sugar levels over a prolonged period [4]. One of the major effects of this disorder is impaired wound healing. Patients with diabetes may have relatively minor wounds such as small cuts after trimming a toenail, but minor wounds of diabetic patients often lead to chronic and nonhealing wounds that are liable to get infected. It is highly common for the infected wound to ultimately lead to the need for amputation. Thus, diabetic patients recorded the highest amputation rate of any type of chronic wound [5]. An estimate suggested that admissions for foot infections created 20% of hospitalizations for patients with diabetes and that led to 50% of all nontraumatic lower limb amputations [5]. Also, 25% of patients with diabetes mellitus are expected to have severe foot problems [5].

Causes for altered tissue repair of diabetes mellitus patients consist of cellular, metabolic, and biochemical factors [5]. The proposed solution is to use tissue engineering approach to repair tissue around regions of minor wound of diabetes patients before the development of severe complications that could lead to the amputation of patients. This involves cell seeding of scaffolds with appropriate mechanical properties to enable the regrowth and replacement of destroyed tissue [6].

1.3 Motivation and Justification

Usually, polymer processing technologies are intended for large scale and high quantity production. On the other hand, computer-assisted design and manufacturing can be used to tailor individual parts for special applications. This technology allows for the construction of individual, patient-specific substances such as scaffolds with ideal internal structures [3]. Biomedical scaffolds made from biocompatible and biodegradable polymers can promote cell growth and can also serve as transporters for innovative drug release systems [3].

This technology, as proposed can be used to repair tissue around the wounds of diabetic patients to prevent the eventual risk for amputation due to infection. This solution could possibly reduce the amount of diabetic patient amputations. The viability of this method could also provide an easily way of producing scaffolds.

1.4 Objectives and Expected Outcome

Biodegradable polymers such as, poly(lactic-acid) (PLA), polyglycolide acid (PGA) and or copolymer of polylactic-co-glycolic acid) (PLGA), when incorporated into the 3D

printing process would produce ideal biocompatible and biodegradable scaffolds with controlled porosities and geometries for optimal tissue regeneration.

The following specific objectives would be carried out during this project:

- The use of materials selection techniques for product design would be used to aid the selection of competing materials for the fabrication of the scaffolds. Cambridge Engineering Selector (CES) would be involved at this stage to trait down competing and desired bioengineering materials.
- Design of biodegradable scaffolds will be done using computer aided designs tools (CAD), specifically SolidWorks. The designs will consider different architectural designs with different porosities.
- The CAD information would aid in modelling effective scaffolds and then practically use 3D printing techniques to fabricate the scaffolds.
- Mechanical simulations of the fabricated scaffolds would be investigated with SolidWorks.
- Mechanical characterisation of the samples will be ascertained with universal mechanical testing machines.
- Optical characterization would also be done at regular interval especially during degradation process.
- Biochemical degradation via mass loss over time would be carried out in a phosphate buffer saline solution (PBS) at different pH.
- There is also the potential for scaffolds to serve as carriers for innovative drug release systems. This potential comes from the possibility of modelling complex designs using CAD techniques. This idea would be explored later in this project.
- Results would be validated by comparing to existing literature.

- The implications of the results would then be discussed for the manufacturing of 3D biodegradable scaffolds with optimized mechanical properties, environmental stability, and biocompatibility with desired porosities for tissue regeneration.

1.5 Activities and Timelines

Below is a chart showing the timeline of the project from the research stage to completion of the project. All activities shown were conducted over a period of 7 months, from September of 2018 to April of 2019.

Table 1. 1: *Timeline of Project Activities*

Task	Sept (2018)	Oct (2018)	Nov (2018)	Jan (2019)	Feb (2019)	March (2019)	April (2019)
Problem Statement and Design Criteria.							
Material Selection							
SolidWorks Design							
Fabrication							
Mechanical Characterization							
Report Submission and draft of paper for publication.							

Chapter Two

2.0 Literature Review

2.1 Statistics on Diabetic Mellitus

As of 2014, about 382 million people were diagnosed with diabetes, with over 19 million of them being Africans [7]. These numbers are projected to increase to 522 million people globally, with 41.5 million people been the case in Africa by the year 2030 [7]. Diabetic mellitus patients have altered tissue repair, meaning that minor wounds such as small cuts can become severe and non-healing [5]. This leaves patients prone to infections due to the presence of open wounds. Once a diabetic patient develops a sore or an ulcer, there occurs a breach in the continuity of the skin and the underlying tissue [8]. Suitable care should therefore be administered to prevent infection and ultimately, amputation.

Research paper by David Greenhalgh [5], addressed diabetic cases as highlighted below: Studies conducted on 194 patients with diabetic foot ulcers were being followed for 1 year resulted in 65% healing, 15% requiring amputations, 16% failing to heal, and 4% dying. Moreover, with 64 patients diagnosed with 78 ulcers (some with multiple wounds) being followed for 6 months resulted in 47% receiving healing, 22% requiring amputations, 22% failing to heal and 13% of the patients died. Also, in a third sample, patients from 10 independent wound healing trials were selected and it was found that in the sixth trials that followed patients for 20 weeks, 31% were healed. For the fourth trials, patients were followed for 12 weeks and 24% of the control patients were healed [5]. From these numbers above, 20% of the sample size of patients either die from their sore or don't get healed.

These numbers are meant to reflect the part of developed world. It is a good guess to estimate that the percentages of people that don't get healed of their sores and or die are much greater in Africa. Ways to reduce these numbers depends on educating the public on the prevention

of diabetes mellitus and engineering skin tissue to grow over and heal open wounds of diabetic patients.

2.2 Possible Diabetics Interventions

According to the Ghana standard treatment guidelines on large chronic ulcers, either pharmacological or non-pharmacological approaches are required to treat sores. For the non-pharmacological approach, the sore must be kept clean with saline solution over a period depending on the intensity of the wound [8]. For the pharmacological approach, antiseptics such as chlorhexidine or cetrimide along with specific antimicrobial treatments are used to aid in the treatment of ulcer [8]. As mentioned in section 2.1, there is a possibility for diabetic patients to maintain their ulcers throughout their treatment and this makes these patients prone to viruses and infections due to open sores.

Tissue engineering for skin regeneration is an option to treat open wounds on diabetic patients. Tissue engineering has the possibility to restore diseased or damaged tissues with no need for organ donors. The extreme disproportion between suitable donor organs and transplant patients have averagely left more than 100,000 people waiting for organ transplants [6]. This has also created an estimated of 19 people dying every day, while waiting for an organ transplant [6]. Tissue engineering has the potential to overcome the current challenges.

During tissue engineering for skin regeneration, grafts are made with the necessary harvested skin cells and seeded into scaffolds, allowing the tissue to generate over time within the scaffold (as the scaffold disintegrates simultaneously) [2,6,18]. This makes scaffolds a very important part of skin regeneration. The scaffolds used in tissue engineering are designed to have similar if not the same structural, chemical and mechanical properties of the bodies' natural extracellular matrix [6]. For this to be achieved, protein fibers are

woven in a network of chains to support tissue mechanically and transfer external mechanical stimuli to the cells. Hence, the cells use that information to produce molecular signals [6]. Scaffolds must therefore maintain suitable chemistry for cell-scaffold interaction, mechanical integrity, biocompatibility, and maintained ideal degradation at a rate equivalent to the skin tissue without loss in function [2,6,18].

2.3 Conventional Methods for Scaffold Fabrication

2.3.1 Solvent Casting

This method is usually combined with particulate leaching. Thus, it involves casting with water soluble particulates into molds. The particulates are leached away using water or any other suitable solvent as pore forming agents in the scaffold [2,9].

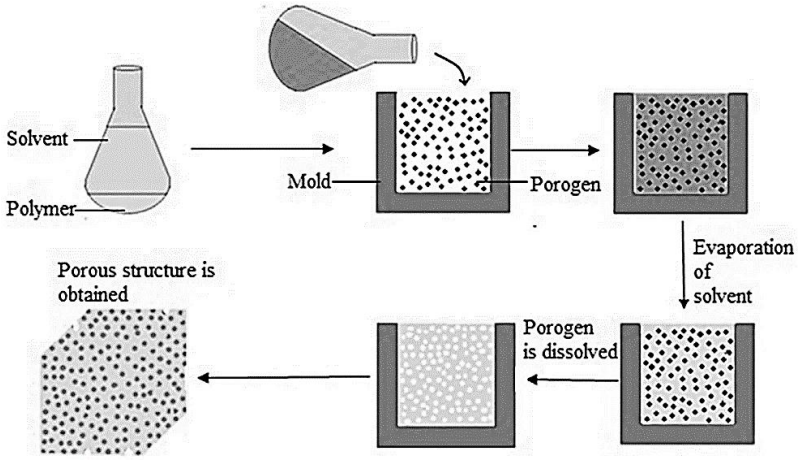

***Figure 2.1**: General method of solvent casting [9].*

2.3.2 Electro spinning method

This method involves the formation of functional fibers with various additives through the co-spinning of PGA and PLA fibers in combination [2,10]. This is commonly used to control the rate of scaffold degradation [2]. These polymers are also combined with other polymers to increase the biocompatibility of the scaffold [2].

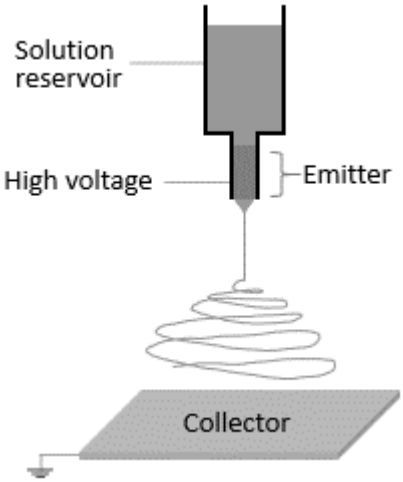

***Figure 2.2**: Electrospinning Schematic [10].*

2.3.3 Phase Separation Technique

This method is dependent on the principle homogeneous multicomponent system whereas a polymer-water emulsion develops thermodynamic instability and separates to lower the free energy [2]. This phase separation technique which is thermally induced forms a polymer-rich and a polymer-lean phase [2]. The formation of the scaffold is by the lyophilization or solvent evaporation of the polymer-rich phase [2]. Parameters such as type of polymers and their viscosity, type of solvent and its volatility, quenching temperature, gelling time, etc. determine the structure of the scaffold [2].

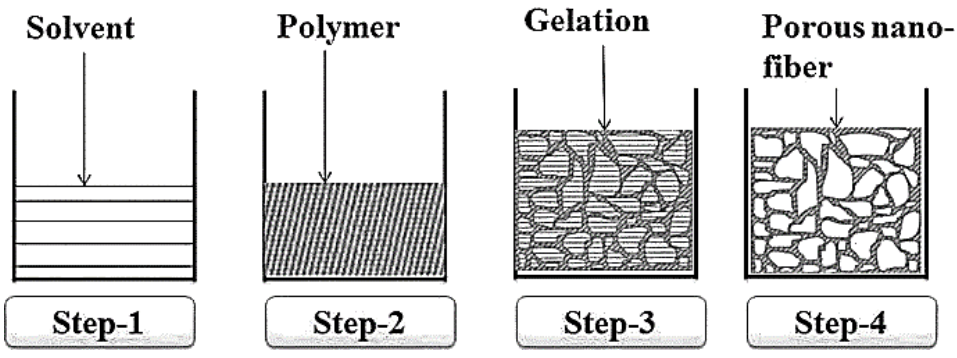

***Figure 2.3**: Process of Phase Separation Technique [11].*

2.3.4 Solid Free-form Fabrication

This method is known as rapid prototyping. It is relatively newer than the methods above [2,9]. In this technique, computer aided design (CAD), computer tomography (CT) and

magnetic resonance imaging (MRI) technology is used to form the 3D model digital information [2,9]. This information is converted to a machine specific cross-sectional format, expressing the model as a series of layers [2]. The file is then implemented on a solid freeform fabricate (SFF) on machine, which forms 3D objects by layered manufacturing strategy [2,9].

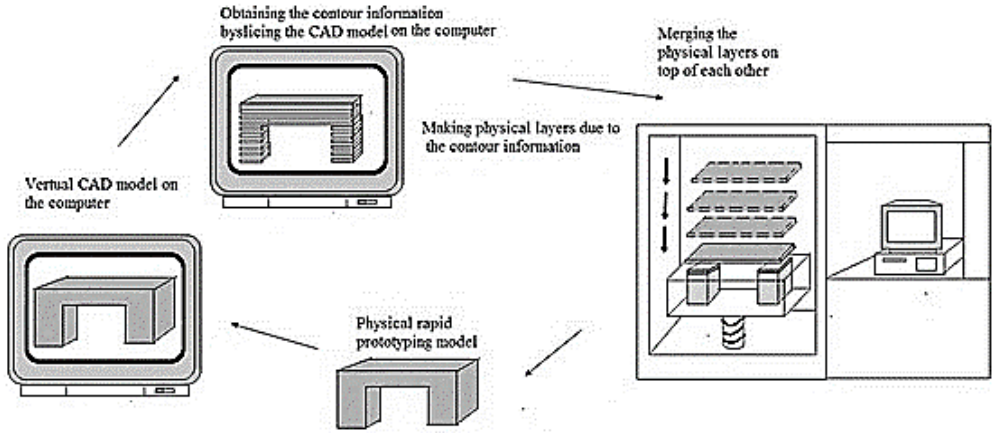

***Figure 2.4**: Solid Free-Form Fabrication (SFF) schematic [9].*

As the objectives of this project implied, a method like solid freeform fabrication would be explored. Using a 3-dimensional (3D) printer to print out the designed scaffold which would be created using CAD techniques, in SolidWorks software. 3-D scaffolds will also be fabricated via solvent casting.

2.4 Unresolved Issues

This section discusses factors that contribute to the difficulty in diabetic wounds healing. These factors can be categorized into the following:

a. Diabetic Patient's Behavior

The patient's adherence to treatment is a major factor that affects the recovery of a patient. It has been widely acknowledged by health practitioners that patients with diabetic ulcers

are commonly poor adherers to treatment [9]. This is possibly due to the rigorous, yet recommended treatment regimen.

Another behavioral issue is the patient's mental health. Examples of such mental health issues that can affect treatment are depression and stress [9]. Depression and a reduced quality of life have been noted to be a come along with diabetic ulcers [9].

b. Diabetic Patient's Physicality

Issues with defective healing in patients, infections, ischemia and deformities affect the healing of diabetic ulcers [9]. Defective healing, possibly from impaired immune response and/or ischemia can interfere with the physiological processes that take place when a wound is healing, thus making ulcers hard to heal [9]. The defects from diabetes also slow the healing process, increasing the chance for an infection to occur. Swift identification and classifying of infections from minor, involving 'superficial structures', moderate to severe limb and or life threatening using authorized measures is therefore very important and hard to achieve [9].

c. The Health System in the region

Depending on the region the patient is located, the presence of effective resources, organizational structure, goals and objectives and politics within health systems to aid in the healing of diabetic wounds vary [9]. Health practitioners within the region assigned to undergo treatment may also have varying skills, resources and professional culture [9].

From the unresolved issues listed above, a simple and effective method is required to reduce the difficulties faced by health practitioners. The proposed method is to replace the damaged tissue instead of repairing the tissue by treating the wound, which is the common focus. To do this, scaffolds are needed to guide the growth of the tissue from healthy cells. From the conventional methods of scaffold formation listed above, methods such as solvent casting

and phase separation have one major shortcoming. This is that the health practitioner or fabricator cannot tailor the scaffold to each patient's specific need to optimize the fabrication. On the other hand, other methods that require CAD can be used to tailor the scaffolds. 3D printing techniques is the method of focus for this project.

3D printing techniques are relatively new technology which can be used to fabricate scaffolds for tissue engineering. On the other hand, the mechanical properties of 3D printed materials have not been extensively studied to ascertain the properties of the natural materials. In effect, this work will investigate the effect of processing techniques on the mechanical properties of the scaffolds.

2.5 Scope of Work

The first chapter of this project presents background studies, problem statement, motivation and specific objects for the execution of the project. The second chapter acknowledged the effort of the scientific community for providing the platform to build on. The chapter also presented statistics on the disease, possible diabetics' interventions, conventional methods for scaffold fabricates, and unresolved issues.

The third chapter presents the list of materials and experimental procedures where materials selection techniques would be used for product design to select competing materials for the fabrication of the scaffolds. Cambridge Engineering Selector (CES) would then be involved at this stage to trait down competing and desired bioengineering materials. Biocompatibility and mechanical properties of various materials would also be compared to the properties of the human skin. This is to enable us to select the most suitable materials for the fabrication of the scaffolds to hold the place of missing skin as skin tissue is expected to develop within and eventually the scaffold. The design of the biodegradable scaffolds will be done using computer aided design tools (CAD), mainly SolidWorks. Various designs are to be

developed and these would consider different structural designs with different porosities. Using the CAD information 3D printing techniques would be used to fabricate the scaffolds.

Mechanical simulations of the fabricated scaffolds would be investigated with SolidWorks. Mechanical characterization using materials testing machines will be carried out to validate the simulated results on their mechanical properties. Biodegradation via biochemical process at different pH would be studied. Thus, these tests include biochemical degradation via mass loss over time in a phosphate buffer saline solution (PBS) at different pH. Optical characterisation would be carried out to determine the pore-density of the fabricated scaffolds.

The fourth chapter presents the results and discussion section while discussing the implications of the results for the fabrication of bioengineered scaffold with optimum mechanical, chemical, and optical properties to stand the test to be used for wound healing. Concluding remarks and recommendations are therefore discussed for future works in the fifth chapter.

Chapter Three

3.0 Methodology and Design

3.1 Design Requirements

Table 3.1 below shows the accepted requirements for the design of the scaffolds.

Table 3. 1: Table of Design Requirements [14]

Requirements	Description
Geometry	The scaffold must fill the space of the defect to guide the tissue regeneration process to completely replace the damaged tissue.
Bioactivity and Biocompatibility	To avoid complications when in close contact to human tissue and to support cellular activity without affecting the host tissue.
Biodegradability	As it is meant to be a provisional structure, the scaffold must degrade over time leaving the tissue formed in its place.
Porous structure	This is to allow for cell penetration and nutrient transport during tissue regeneration.
Mechanical capability	The mechanical performance of the scaffold must be sufficient to withstand implantation handling and support the loads and stresses applicable.
Fabrication	The scaffold should be tailored to the diseased / injured area.
Commercialization	The scaffold should be produced with an automated and reproducible technique.

3.2 Materials Selection

The main criteria for the selection of materials for the fabrication of the scaffolds were as follows:

- Biocompatibility
- Yield strength or elastic limit and
- Young's Modulus

For these properties, the human skin was used as the baseline since the application of the scaffolds are targeting skin repair. With the use of CES EduPack 2013 material selector software (Granta Design, Cambridge, United Kingdom), possible materials for the

project were selected. With CES software, plots were obtained for Young's modulus versus yield strength for possible selection of biocompatible polymers for human skin. With the selected materials, graphs for comparing each material's yield strength and Young's modulus were also developed. Polylactide (PLA) and polylactic-glycolic acid (PLGA) were the best computing candidate to be considered for the study. From that, Pugh matrix was formed.

Similarly, from Figure 4.3, PLA and PLGA have higher yield strengths than the human skin. This means that they can withstand more force before tearing as compared to the human skin.

***Table 3.2**: Pugh Matrix for PLGA and PLA alternatives.*

	Baseline	**Alternatives**	
Criteria	**Human Skin**	**PLGA**	**PLA**
Biocompatibility	Yes	1	1
Young's Modulus	0.001-0.05	1	1
Yield strength	0.6-1.3	1	1
Printability	-	1	1
Availability of Filament (not expensive)	-	1	0
Total		5	4

It shows that these materials can serve as replacement for the skin by comparison. On the other hand, other properties such as optimum working temperature and degradation rate over time could bring out the difference between PLA and PLGA. These two alternatives are good enough to be used for the fabrication of the scaffolds. PLA is

commonly used for 3D printing and it's less expensive. It is also good for this application as it does not require impact strength or tolerance to heat loads [10].

3.3 Design of Scaffold

The effectiveness of the application of scaffolds depends on many features as shown in Table 3.2, but this section focusses on the scaffold architecture. The architecture consists of both the dimensions and pore size of the scaffold. The design of the scaffold was conducted in SolidWorks as shown in Figure 3.1. The overall thickness comprised of approximately 1.5 mm, length of 5 cm and breadth of 5 cm. As also shown in Figure 3.1b and 3.1c, the design consists of arrays on cylinders in perpendicular directions. Each cylinder has a diameter of 0.5 mm and is approximately 0.2 mm away from the next cylinder. This arrangement creates a porous body with pore diameter of approximately 0.2 mm. The PLA filament was procured from . Ultimaker 2 Extended^{+} 3D printer (Serial number: 9206, Netherlands, Ultimaker) and a PLA filament of 2.8 mm diameter were used to execute the printing of the scaffolds.

Since this scaffold is intended for human skin regeneration, the dimensions of the scaffold would need to mimic that of the human skin. The thickness of human skin can vary due to the age and the location on a person's anatomy. The skin on a person's palms and the feet soles are thickest and the skin on a person's eyelids is the thinnest [11]. The skin of males is also naturally thicker than that of females in all body parts. The skin tissue of a person could range from 0.05 mm to 1.5 mm [11]. For this project average skin thickness is assumed from this range to be 1.5 mm. The length and breadth of the scaffold could vary depending on area of application. For this project, 100 µm macrospore diameter was used.

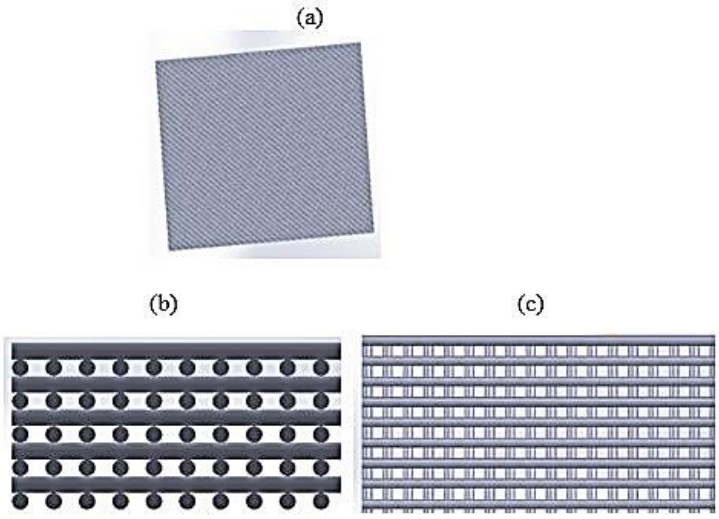

Figure 3. 1*: SolidWorks Design of PLA Scaffold, (a) Full View, (b) Side View, and (c) Top View.*

One of the design requirements of this scaffold was commercialization or automated and easy production. From the model shown in Figure 3.1, the volume of the spaces within the structure where the cells can attach, and grow were calculated by [12] :

$$V_{space} = V_{structure} - V_{total} \tag{3.1}$$

where V_{space} is the volume of space, $V_{structure}$ is the overall volume of the structure, and V_{total} is the total volume of the cylinders.

Given that human skin cells are flat and range from 25-40 microns squared [12], the number of human skin cells that can fit in above volume is determined from equation (3.2) [12]:

$$Number\ of\ cells = \frac{Volume\ of\ space}{[(area\ of\ skin\ cell)(thickness\ of\ structure)]} \tag{3.2}$$

$$= \frac{2.19 \times 10^{-6}}{[(25 \times 10^{-6})(1.5 \times 10^{-3})]}$$

$$= 58.4\ cell$$

3.4 Experimental Procedures

Validation of the results obtained from the 3D printed scaffolds was done by manually fabricating 3D scaffolds via solvent casting, for comparison. For this experiment, two types of scaffolds were casted. One made purely from PLA and the other made of both PLA and PEG with a 1:1 ratio.

During the process, 9 g of polymer samples, PLA and PEG were dissolved with dichloromethane and distilled water, respectively. 2 ml of each polymer solutions were separately casted into mini-Petri dishes. Fine particles of salts/sugar were then dropped gradually into the polymer solutions until saturation. The samples were then allowed to dry for 6 h. Samples were then removed carefully and let into large volume of water to leach out the salt/sugar particulates. The solution was then replaced until all residue of the sugar/salt were removed. This is always observed by samples floating at the top of the water. Samples were then characterized to ascertain the effect of processing method and the mechanical properties of 3D scaffold to provide solution for the treatment of recurring wounds.

Table 3. 3: *Table of Materials to be used for Solvent Casting*

Purpose	Material to be used
Polymer	1G of PLA / 5G of PEG
Porogen	Salt / Sugar
Solvent	1L Dichloromethane

3.4.1 Tensile and Compressive Test

Tensile test provides the force the sample can withstand before increasing in length or elongating. The compressive test provides the force the sample can withstand before decreasing in length. Using a tensile testing machine, as shown in the setup in Figure 3.2, the samples were stretched to determine their elastic and plastic properties. For this test, 5 samples of the 3D printed scaffolds were placed in the machine to be tested. The results collated for each sample were the modulus of elasticity, the peak load, the peak stress recorded and the sample strain at its failure or break. Comparison were made by similar test with the solvent casted 3D samples.

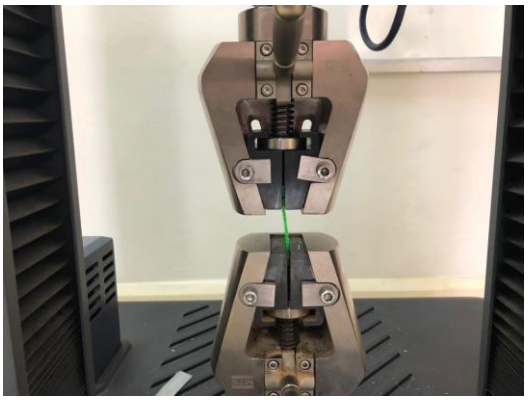

Figure 3. 2: *Tensile Test setup.*

3.4.2 Stiffness test

This is also known as a flexural strength or a 3point bend test. Flexural strength with a 3-point bend test was virtually conducted on SolidWorks with the design samples. The results were validated with a universal testing machine. For this test, the flexural modulus, the flexural strength and the yield point were evaluated. These were compared to the literature.

The flexural modulus measures the stress/strain of the samples and indicates the stiffness of the samples [13]. The flexural strength and yield point measure the maximum load the samples can withstand before failing [13].

Using a tensile testing machine, as shown in the setup in Figure 3.3, the samples were stretched to determine their elastic and plastic properties. For this test, 5 samples of the 3D printed scaffolds were placed in the machine to be tested. The results collated for each sample were the modulus of elasticity, the peak load, the peak stress recorded and the sample strain at its failure or break. Comparison were made by similar test with the solvent casted 3D samples.

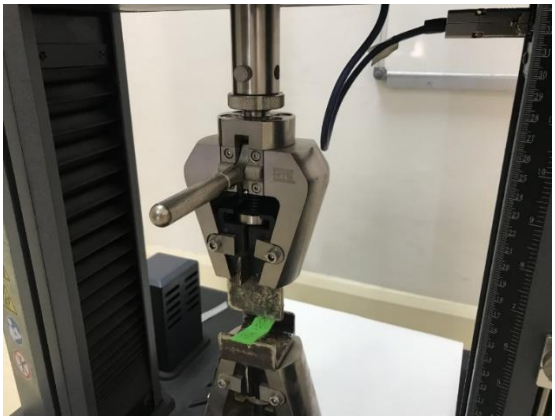

Figure 3. 3: *3 Point Bend Test Setup*

3.4.2 Mass Loss Degradation test

Biochemical degradation via mass loss over time would also be carried out in a phosphate buffer saline solution (PBS) at different pH levels. This would be done for both 3D printed and solvent casted samples. To create the environments where the samples would be placed, buffer solutions of pH 4.0 (produced by Reagecon), 7.0 (produced by Reagecon) and 10.0 (produced by DAEJUNG) along with HCl and NaOH were used to adjust and create the optimum temperatures for the test.

Two samples each were placed in solutions of pH 4.0, 7.0 and 7.4 as shown in Figure 3.4. These samples were left over a period of 4 days and observations on the mass of the samples before and after being placed in the pH environments were made. Filter papers (produced by Xinxin) were used to drain the solution absorbed by the sample from them before being weighed using a mass balance (produced by Highland).

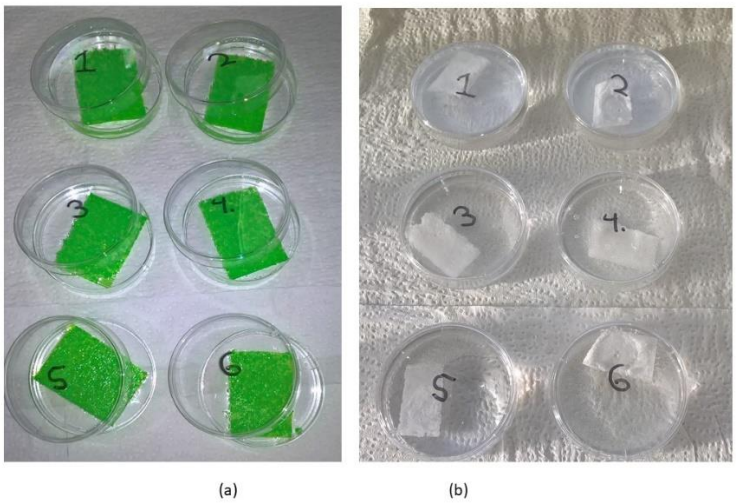

Figure 3. 4: *Mass loss Degradation Test Setup (a) 3D Printed and (b) 3D Casted Scaffolds*

3.4.2 Hardness Test

For this project, a hardness test would also be undertaken to obtain more mechanical properties of the fabricated scaffolds. A shore d durometer (Digital Shore D Hardness Durometer, 16HDM002-D100HD-06, Yescom USA, California, USA) would be used to conduct the hardness test. Hardness testing is done to determine the resistance a material shows to permanent deformation by penetration of another harder material [14]. In the process of testing the hardness of the scaffolds, the scaffold is placed down flat on a surface and the tester is pressed down on the scaffold, perpendicular to the scaffold. The setup is shown in Figure 3.5 below.

Figure 3. 5: *Shore D Durometer*

Chapter Four

4.2 Results and Discussion

4.1 Materials Selected with CES Software

CES result obtained (Fig. 4.1a) from the sorted materials with the criteria of biocompatible polymers, yielded polylactide (PLA) and polylactic-glycolic acid (PLGA) as optional materials to be selected for the 3D scaffolds fabrication. These materials are both biocompatible. Using the CES material selector software, each material's yield strength and Young's modulus were also presented (Fig. 4.1b). From this graph (Fig. 4.1c), the Young's modulus of PLGA and PLA are higher than that of human skin making these materials stiffer than the human skin. Thus, the selected materials are less elastic, when compared to skin. Thus, more force is required to change the shape of these materials. However, the tendency of the selected materials (PLA, PLGA) to degrade at physiological conditions (pH 7.4 and 37℃) makes them suitable as they are likely to experience reduction in mechanical properties to levels that could matches with the skin.

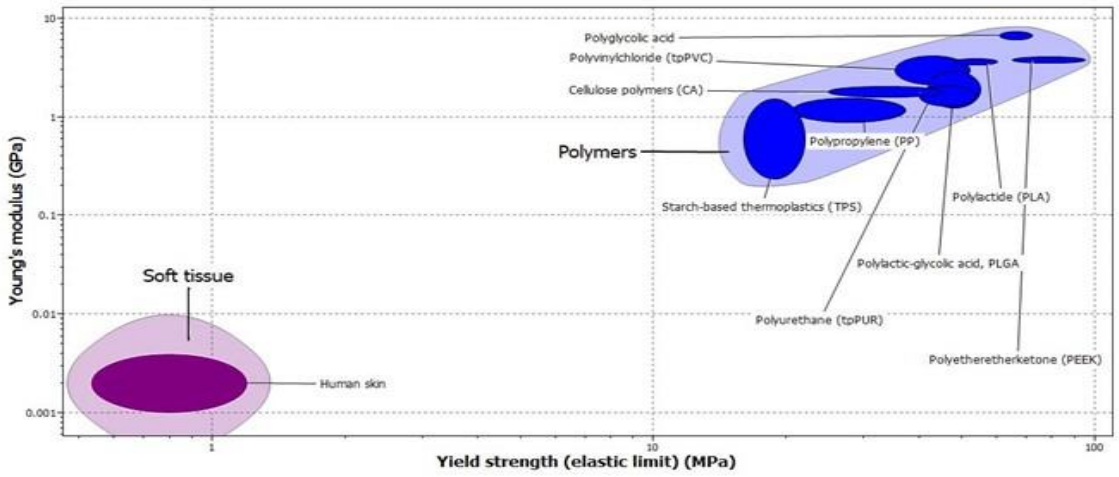

(a)

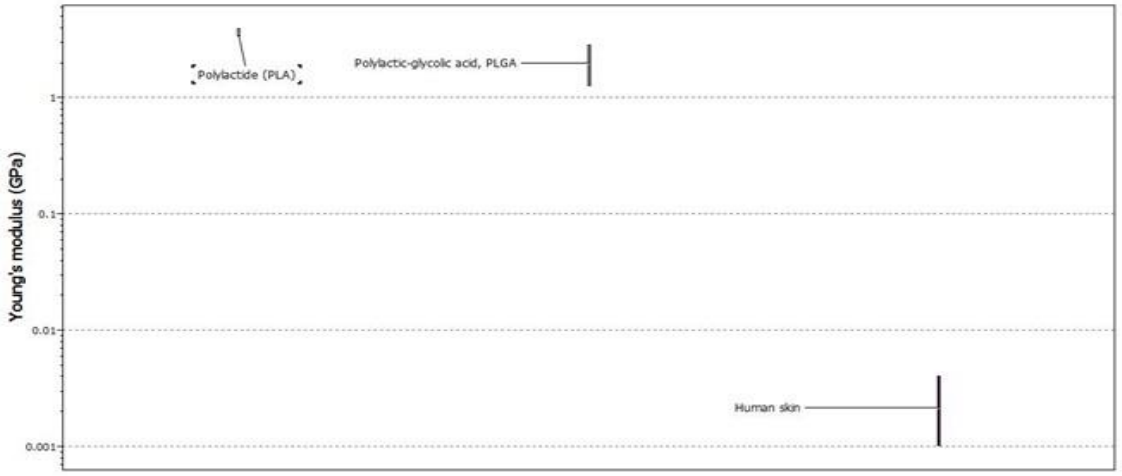

(b)

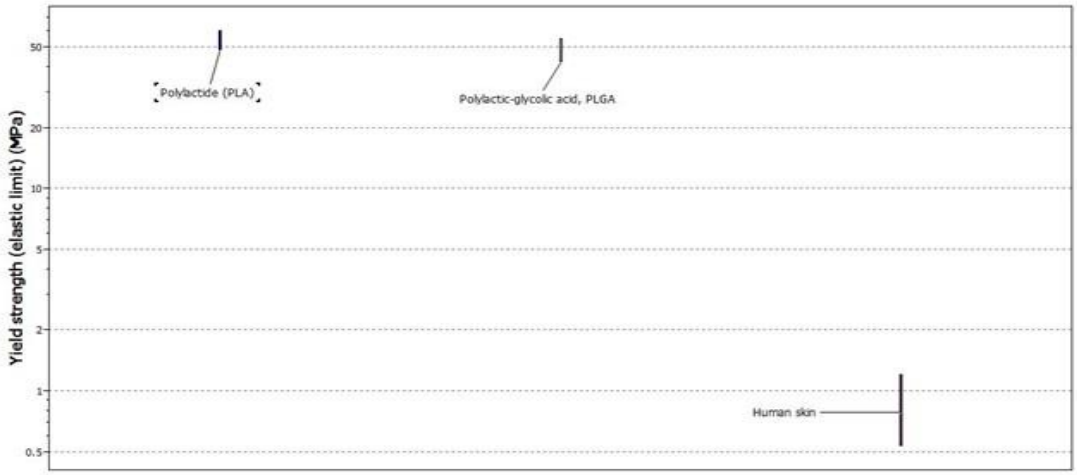

(c)

Figure 4. 1: *CES Result: (a) Young's Modulus versus Yield Strength of Human Skin and Biocompatible Polymers, (b) Comparing the Young's Modulus of PLA, PGA and Human skin, and (c) Comparing the Yield Strength Comparison of PLA, PGA and Human skin.*

4.2 Optical Characterization of 3D Printed Scaffolds

Using a digital microscope (model U200X, made in China) as a poroscope, the porosity of the 3D printed, and casted scaffolds were investigated. Below are images of 3D printed scaffold from the design matrix (Fig. 4.2). Pores sizes of the scaffolds is important for appropriate guidance of cell to cell and cell to scaffold interaction as it influences cell adhesion, movement and propagation [15]. Due to this, pore sizes can influence different cell processes. Macropores have an important role in cell seeding, distribution, migration and further neo-vascularization in living organisms. For skin tissue regeneration to effectively be achieved, scaffolds with macropores are needed. Macropore diameters range from 100 µm (0.1 mm) to 1 mm [15]. The optical images of the solvent casted scaffolds are also presented in Figure 4.2 (c-d).

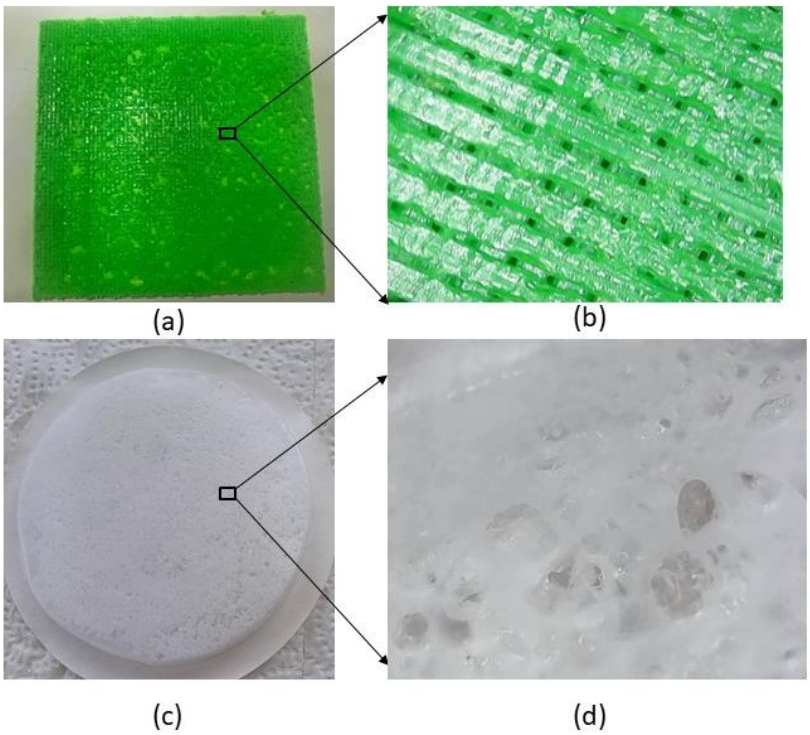

Figure 4. 2: *Optical Images of Scaffolds: (a) Full View of PLA 3D Printed, and (b) Microscope view of PLA 3D Printed, (c) Full View of PLA 3D Solvent Casted Scaffold, and (d) Microscope View of PLA 3D Solvent Casted Scaffold.*

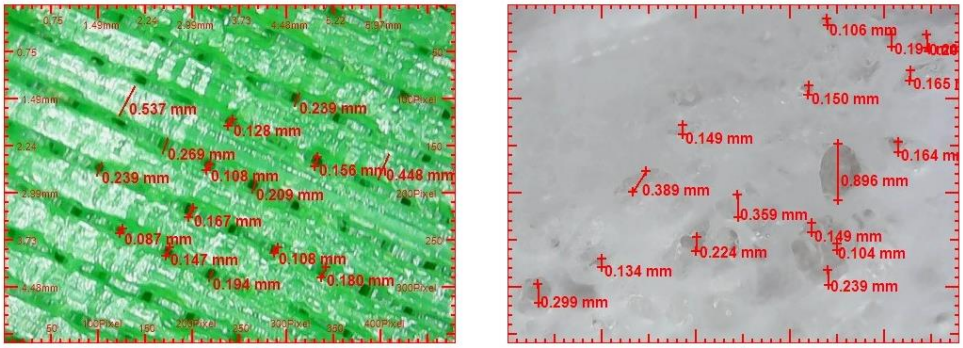

Figure 4. 3*: Optical Images of Scaffolds: (a) Measured pore sizes for Microscope view of PLA 3D Printed, and (b) Measured Pore sizes for Microscope view of Solvent Casted Scaffold*

The printed sample shown above (Fig. 4.3 a) has dimensions that vary from the SolidWorks design. This shows that the errors from the printer used need to be accounted for in the design. Figure 4.2 (a-b) shows that the cylinder diameters and spacing's are on average approximately 0.5 mm and 0.2 mm, respectively.

The CAD software (SolidWorks) used for the design of the scaffolds has a flaw which makes it difficult to create large linear patterns at once. Using the "equations" feature, which in this case was used to make dimensions such as the spacing between each cylinder and the number of cylinders put in the array dependent on the length of each cylinder, the diameter of each cylinder and the overall height of the structure. This feature along with the automated characteristic of a 3D printer make this fabrication method more commercial than others.

Figure 4.3 shows that there is a distribution of varying pore sizes across both the 3D printed scaffold and solvent casted scaffold. Table 4.1 and Figure 4.4 below show the distribution across a portion of both scaffolds.

Table 4. 1: *Pore Diameter sizes on (a) 3D printed Scaffold and (b) Solvent Casted Scaffold*

3D Printed Scaffold (a)		**Solvent Casted Scaffold (b)**	
Pore Diameter	**Count**	**Pore Diameter**	**Count**
0 – 0.10	1	0 – 0.10	0
0.11 – 0.20	8	0.11 – 0.20	9
0.21 – 0.30	4	0.21 – 0.30	3
0.31 – 0.40	0	0.31 – 0.40	2
0.41 – 1.0	0	0.41 – 1.0	1

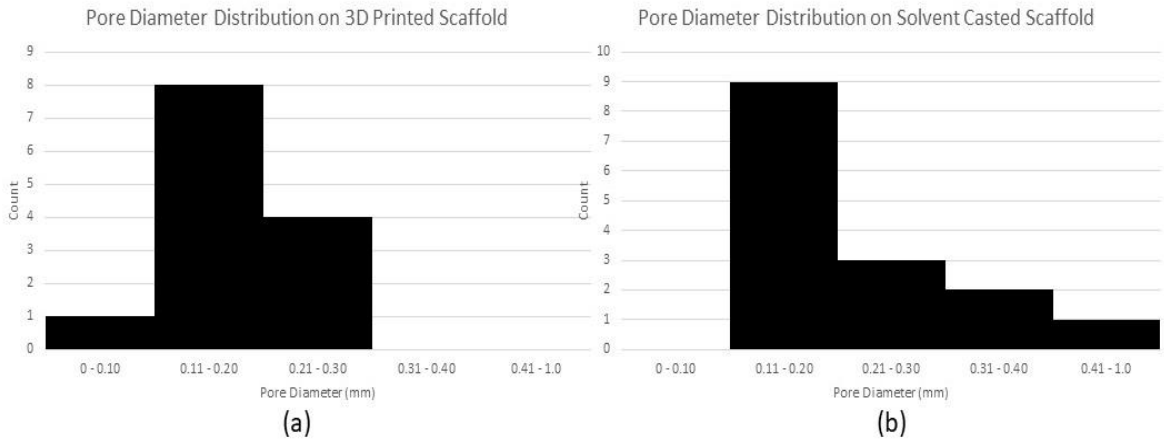

Figure 4. 4*:Pore Diameter size distribution on (a) 3D printed Scaffold and (b) Solvent Casted Scaffold*

4.3 Mechanical Characterization

In this section, stiffness tests along with tensile and compressive tests are undertaken on samples of the 3D printed scaffolds. These tests were done to validate the mechanical properties of the actual 3D printed samples. Figure 4.5 shows 3D printed and 3D casted samples for the mechanical characterization. These samples have the following dimensions:

Table 4. 2: *Dimensions of Samples*

Scaffold	Length (mm)	Width (mm)	Thickness(mm)
3D Printed (PLA)	5.00	10.0	1.50
3D Casted (PLA)	7.00	10.0	3.00
3D Casted (PLA and PEG)	8.00	10.0	3.00

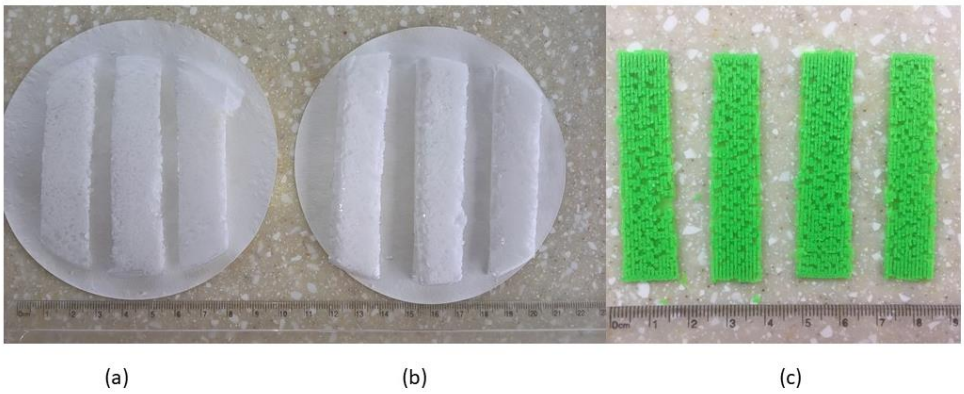

Figure 4. 5: *Tensile test and Stiffness test samples: (a) 3D Casted scaffolds (PLA), (b) 3D Casted Scaffolds (PLA and PEG) and (c) 3D Printed scaffolds*

4.3.1 Tensile Test

The purpose of this test is to find the modulus of elasticity of the PLA 3D printed scaffold by finding the average modulus of the samples. The test was also done to determine the average maximum elongation of the scaffold and the average maximum load it can bear. These results for the tensile test on the 3D printed samples are shown in Table 4.3 below.

Table 4. 3*: Table of Tensile Test Results for 3D Printed (PLA) Samples*

Sample	Modulus of Elasticity (MPa)	Peak Load (kN)	Maximum Elongation(cm)
1	239	0.034	0.045
2	50	0.009	0.105

3	86	0.035	0.120
4	194	0.054	0.105
5	111	0.031	0.090
Average	136	0.033	0.093

The results show that the 3D printed scaffold fabricated could withstand an average peak load of 0.33 kN and attain an average maximum elongation of 0.093cm. The scaffold also has an average elastic modulus to be about 136 MPa**.**

One major source of errors comes from the layout of the fabricated samples. There are inconsistencies of the sample sizes and spacing's along with some gaps of empty space where PLA should be, as shown in Figure 4.5. This makes some parts of the samples stronger than others causing a difference in values shown in Table 4.3.

Table 4.4 below shows the results from the tensile test for both solvent casted samples (PLA only and PLA with PEG). From the results below, both solvent casted samples have the same tensile properties.

Table 4. 4: *Table of Tensile Test Results for 3D Casted Samples*

Sample	**Modulus of Elasticity** $(\boldsymbol{MPa})$	**Peak Load** $(\boldsymbol{kN})$	**Strain**
PLA	133.3	5.0	0.149
PLA and PEG	133.3	5.0	0.149

These results show that the addition of PEG to the sample, making it a composite, does not change the tensile properties of the scaffold.

4.3.2 Stiffness Test

The purpose of this test is to find the flexural modulus, the flexural strength and the yield point of the samples. The results for the bend test conducted on the 3D printed samples are shown below in Table 4.5.

***Table 4. 5**: Table of Bend Test Results for 3D Printed (PLA) Samples*

Sample	**Flexural Modulus (MPa)**	**Peak Load (N)**
1	0.375	2.75
2	0.500	3.20
3	0.300	1.25
4	0.250	3.25
5	0.330	4.75
Average	0.351	3.04

The results show that the samples of 3D printed scaffolds could withstand an average load of 3.04 N and had an average flexural modulus of 0.351 MPa. Just as for the Tensile test, there were inconsistencies in of the sample sizes and spacing's along with some gaps of empty space where PLA should be. This led to the variations in results obtained in Table 4.5, shown above.

Table 4.6 below shows the results from the tensile test for both solvent casted samples (PLA only and PLA with PEG).

***Table 4. 6:** Table of Bend Test Results for 3D Casted Samples*

Sample	**Flexural Modulus (MPa)**	**Peak Load (N)**
PLA	0.67	8.0
PLA and PEG	0.20	7.1

The results above show that the addition of PEG to the scaffold composition reduces the flexural modulus of the scaffold. This makes the scaffold much more flexible.

4.3.3 Hardness Test

The purpose of this test is to determine the resistance the fabricated scaffold exhibits to external forces. This test is done on both the 3D printed and casted scaffolds. The results of the test are shown in Table 4.7 below. The test was conducted on 5 different parts of a sample to find the average hardness of each sample.

Table 4. 7: *Hardness Test Results*

Sample	1	2	3	4	5	Average (HD)
3D Printed (PLA)	16	15	16	17	14	15.6
3D Casted (PLA)	14	17	16	11	15	14.6
3D Casted (PLA and PEG)	3	3.5	2	7	4	3.9

The results above show that the relative Hardness of the fabricated scaffolds is low (below 20 HD). The addition of PEG further decreases the hardness of the scaffold. This is good as the scaffold's hardness can be tailored to suit the need.

4.4 Mass Loss Degradation Test

The purpose of this test was to find the degradation rate of the scaffold samples under 3 different pH environments (20ml solutions). The pH values considered for this test were 7.4 for the pH of human blood, 7.0 as a neutral environment and 4.0 to observe the degradation under acidic conditions. Table 4.7 below shows the results for mass change over a period of 4 days for the 3D printed scaffolds. These results also show the mass of

both wet and dried samples when removed from the pH solutions. This was done to also observe the amount of solution that could be absorbed over the same period.

Table 4. 8: *Mass Change over 4-day period for 3D Printed Scaffolds*

		Mass (g) after 4 days	
Initial Mass (g)	**pH**	**Wet**	**Dry**
0.84	7.4	1.16	0.84
0.88	7.4	1.21	0.88
0.77	4.0	1.15	0.77
0.83	4.0	1.12	0.82
0.87	7.0	1.23	0.87
0.74	7.0	1.19	0.74

From the results above, it is hard to tell if there was any mass change below 0.01 grams as the mass balance used is restricted to 2 decimal places. On the other hand, it is noticed that over the period of 4 days, one of the samples placed in pH 4.0 has lost mass of 0.01 grams. From this result, if the mass loss occurs linearly with time, it can be estimated that it would take $\frac{0.82}{0.01} \times 4days = 328\ days$ for that sample to degrade.

This test was also conducted on 3D casted samples, one made from purely PLA and another of an equal mixture of PLA and PEG. This was done to make deductions on the addition of PEG to the scaffold. Table 4.8 shows the results for this experiment.

Table 4. 9: *Mass Change over 4-day period for 3D Casted Scaffolds*

			Mass (g) after 4 days	
Material	**Initial Mass (g)**	**pH**	**Wet**	**Dry**
PLA	0.35	7.4	1.23	0.35
PLA and PEG	0.45	7.4	1.27	0.45
PLA	0.46	4.0	0.85	0.46
PLA and PEG	0.50	4.0	0.93	0.49
PLA	0.49	7.0	0.81	0.49
PLA and PEG	0.41	7.0	0.78	0.41

Just as seen in Table 4.8, the scaffolds degrade faster under acidic conditions. The addition of PEG to the scaffold does not seem to affect the degradation mechanics of the samples.

4.5 SolidWorks Simulation (FEA analysis)

Using the simulation extension on the SolidWorks software, a test was run on the scaffold design to gain insight on whether the structure can withstand the forces acted on it in its real-world application. The effects on the structure were also noted. For this test, the main force considered is the force exerted by the cluster of skin cells formed within the structure on the walls of the structure. This force considered is the total weight of enough skin cells to fill the scaffold, pushing on the sides of the scaffold.

When the scaffold is applied on a patient, this force acts on all non-fixed sides of the scaffold. For this test the edges of the structure were fixed and a pressure was applied opposite to the fixed edges. For uniform effect across the surfaces the pressure is acting upon and the fixed surfaces, rectangular slabs of PLA were added to the edges of the structure as shown in the figure below.

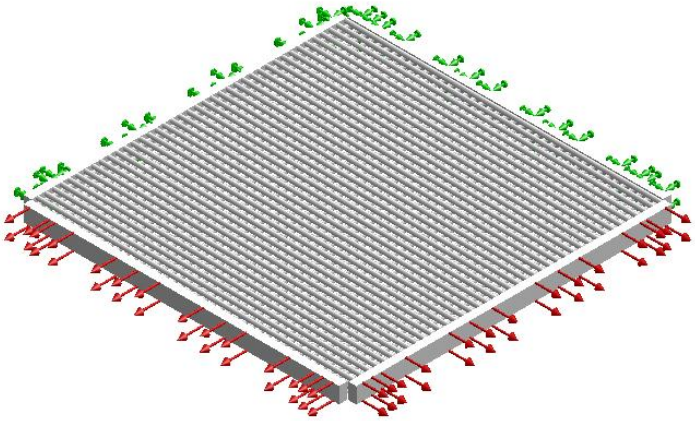

Figure 4. 6: *SolidWorks Model for Simulation.*

The model also has the following properties as shown in Table 4.2.

Table 4.10: *Model Properties.*

Material Properties	**3D Printed PLA**
Tensile strength	30 MPa
Elastic Modulus	2000 MPa
Shear Modulus	3,189 MPa
Poisson's Ratio	0.394
Mass Density	1020 kg/m^3

4.3 Projections of Cells Seeding

The calculations on the number of cells to be seeded on the scaffold was about 58 cells. These cells can fit within the space of the scaffold but when skin cells are formed, the scaffold degrades allowing for the more cells to grow. Assuming there is no degradation and the cells continue to grow, this simulation checks to see if the scaffold would still hold. Given that the mean mass of a cell is 1 nanogram making the mean weight of a cell to be 9.81 micro-Newtons which is very small. If the cells were to be so many to produce 1

Newton force per area of the side walls, the following effects would take place on the 3D printed scaffold (Fig. 4.6 a-c).

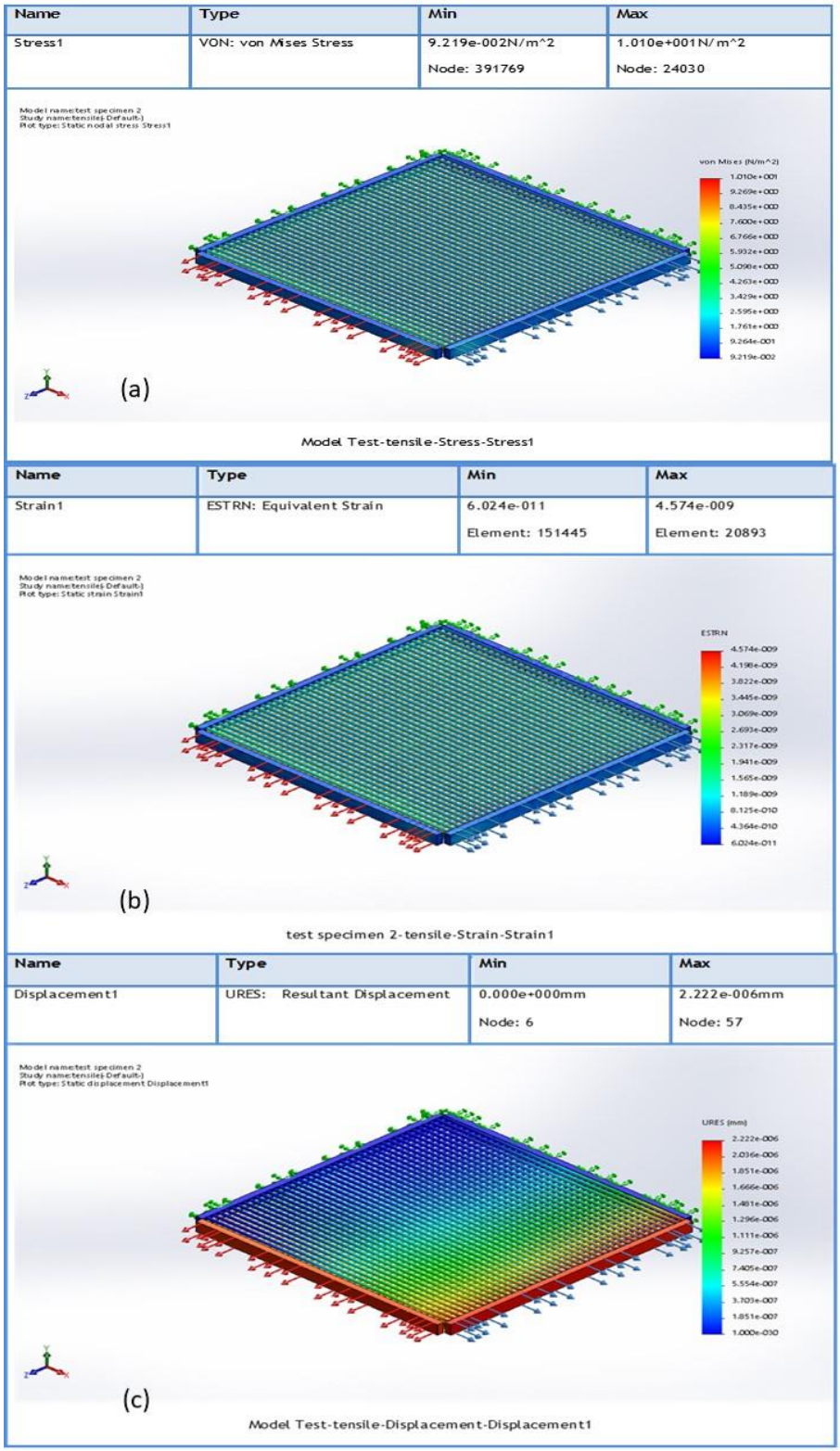

Figure 4. 7: *(a) Von Mises Stress Distribution in model from 1Pa, (b) Strain distribution in model from 1Pa load, and (c) Resultant displacement in model from 1Pa load*

Figure 4.7a show that the force at the upper and lower surfaces of the structure do not experience less stress and strain as compared to the inner surfaces of the structure. This characteristic of the design is good as it leaves the surfaces exposed to the environment (the body of the patient and the air) less affected by the cell formation process and capable of taking on more pressure from the environment.

Figure 4.6c shows that the pressure placed on the structure causes the array of cylinders to stretch by 2.22 μm. However, this stress displacement is not enough for the structure to fail.

These results along with those form Table 4.1 match as these results are far from the maximum possible values. This shows that the model can withstand the forces that would act on it when used on a patient.

5.0 Conclusion

5.1 Remarks and Recommendations

Tissue engineering is an area of exploration to solve the issues of diabetes patient's ulcers. This can be done in the form of skin regeneration to replace the dead tissue on the wound. As functional scaffolds are usually made of biopolymers, this project was focused on the design of these scaffolds using CAD software. The fabrication of these scaffolds using both 3D printing technology and solvent casting, a more conventional method of scaffold formation, was also explored.

Samples were made from these methods, out of PLA and an equal mixture of PLA and PEG. These samples were put under mass degradation tests and mechanical characterization tests. Optical characterization was also undertaken to observe pore size and distribution. From the mechanical characterization tests, it was observed that the 3D printed scaffolds and the 3D casted scaffolds made of PLA had similar results regarding hardness, tensile strength, elastic modulus and flexural modulus. It was also observed that the addition of PLA reduced the flexural modulus of the scaffold, making the scaffolds more flexible and reduced the hardness of the scaffolds.

From the optical characterization, it was observed that using 3D printing to fabricate the scaffolds produced a uniformly arranged distribution of pores. On the other hand, the use of the solvent casting method produced a random distribution of pores and pore sizes ranging from 0.1 mm to 1 mm.

From the results obtained, it can be deduced that 3D printing is the superior fabrication method for scaffold formation as it is easier to create an even distribution of pores on the scaffolds. On the other hand, a biopolymer composed of PLA and PEG would be much more ideal as this would allow for a much more flexible scaffold.

5.2 Limitations

Over the course of this project, there were some limitations that either hindered progress or reduced the quality of the results obtained from testing. Some of these limitations were as follows:

1. 3D print mechanics.

This came from either calibration or in-built settings within the printer of choice. As shown in Figure 4.1 compared to Figure 3.4, the printout of the scaffolds had gaps leaving spaces where PLA was expected to be as shown in the arrangement of Figure 3.4.

2. Lack of an analytical weighting balance with at least 4 decimal places.

   Biological degradation of polymers/scaffolds occurs with minimal loss of materials from the bulk system. This require a highly sensitive equipment. The lack of the required equipment needed to accurately measure the mass loss over time led to unmeasurable changes in mass, and hence yielded to inaccurate results for the biodegradation test.

5.3 Future works

Aside the extensive mechanical characterization on the scaffolds, one major thing to do as a way forward is to undergo cell seeding onto the scaffolds. This test would be used to determine whether the fabricated scaffolds would produce the optimum environment for skin cells to grow and form skin tissue. This process would be undertaken over a 30-day period where cell seeded scaffold samples would be monitored to observe cell activity (whether growth or decay).

As mentioned in the earlier chapters of the paper, scaffold design presents the opportunity to deliver drugs to patients fitted with them. This opportunity was not explored during the period of this project but could be considered in future works to optimize the use

of scaffolds for wound healing. Samples of the scaffolds could also be tested on smaller animals to ascertain tissue regeneration.

References

[1] S. Hollister, "Porous scaffold design for tissue engineering.," *Nature Materials,* p. 518, 2015.

[2] P. K., "Biomaterials for Tissue Engineered Scaffolds," *Advanced Technologies for Enhancing Quality of Life,* pp. 93-94, 2010.

[3] L. Ru¨diger and M. Rolf , "Desktop manufacturing of complex objects, prototypes and biomedical scaffolds by means of computer-assisted 3D plotting of polymers and reactive oligomers," *Macromolecular Materials and Engineering,* p. 17, 2000.

[4] "About diabetes," World Health Organization, 31 March 2014. [Online]. Available: https://web.archive.org/web/20140331094533/http://www.who.int/diabetes/action_online/basics/en/. [Accessed 26 September 2018].

[5] D. G. Greenhalgh, "Wound healing and diabetes mellitus," *Clinics in Plastic Surgery,* pp. 37-38, 2003.

[6] J. W. Drexler, Materials Engineering for Enhanced Tissue Scaffold Mechanical, The Ohio State University, 2010.

[7] V. O. Adjei Salia, Experiences of Indviduals living with Diabetic Foot Ulcers at the Korle Bu Teaching Hospital, Accra, Ghana: University of Ghana, 2014.

[8] "Medicines Policy for Selected African Countries," World Health Organization, [Online]. Available: http://collections.infocollections.org/whocountry/en/d/Js6861e/10.3.4.html. [Accessed 30 October 2018].

[9] V. Nube, G. Frank, J. White, S. Stubbs, S. Nannery, L. Pfrunder, S. M. Twigg and S. V. McLennan, "Hard-to-heal diabetes-related foot ulcers: current," *Chronic Wound Care Management and Research,* pp. 134-141, 2016.

[10] www.sd3d.com/materials, *PLA Technical Data Sheet,* SD3D.

[11] B. Amirlak, "Skin Anatomy," *Medscape,* 2017.

[12] P. M. R. Wilkinson, in *Skin*, Cambridge, Cambridge University Press., 2009, pp. 49-50.

[13] A. DeWolfe, "How to Perform a 3 Point Bend Test on a Universal Testing Machine," Adamet Materials Testing System Manufacturer, 23 July 2010. [Online]. Available: https://www.admet.com/how-to-perform-a-3-point-bend-test-on-a-universal-testing-machine/. [Accessed 18 January 2019].

[14] Y. Hayakawa, A. Chen, K. Ishikawa and C. Zhen, "Hardness Testing," Stuers, [Online]. Available: https://www.struers.com/en/Knowledge/Hardness-testing. [Accessed 22 April 2019].

[15] I. Bružauskaitė, D. Bironaitė, E. Bagdonas and E. Bernotienė, "Scaffolds and cells for tissue regeneration: different scaffold pore sizes—different cell effects," *Cytotechnology - PMC,* 2016.

[16] C. Guoping , U. Takashi and T. Tetsuya, "Scaffold Design for Tissue Engineering," *Macromolecular Bioscience,* pp. 69-72, 2002.

[17] U. T. G. Sampath, Y. C. Ching , C. . H. Chuah, J. J. Sabariah and P.-C. Lin, "Fabrication of Porous Materials from Natural/Synthetic Biopolymers and Their Composites," *Materials,* vol. 9, no. 12, 2016.

[18] "nanoScience," nanoScience instruments, [Online]. Available: https://www.nanoscience.com/techniques/electrospin/. [Accessed 02 01 2019].

[19] "Biomaterials-based nanofiber scaffold: Targeted and controlled carrier for cell and drug delivery," Researchgate, December 2014. [Online]. Available: https://www.researchgate.net/figure/Illustration-of-the-production-process-of-nanofibers-by-phase-separation-technique_fig5_270003403. [Accessed 02 January 2019].

[20] B. Kale, "Biocompatible Polymers," 2 March 2013. [Online]. Available: https://www.slideshare.net/birudevkale/bk-ppt1.

[21] F. Baino, G. Novajra and C. Vitale-Brovarone, "Bioceramics and Scaffolds: A Winning Combination for Tissue Engineering," *Frontiers in Bioengineering and Biotechnology,* vol. 3, p. 2, 2015.

Appendix

Appendix A

Calculations of volume of space within the structure where the cells can attach is calculated as:

$$V_{space} = V_{structure} - V_{total} \quad (3.1)$$

where V_{space} is the volume of space, $V_{structure}$ is the overall volume of the structure, and V_{total} is the total volume of the cylinders.

Henced,

$$V_{space} = [(5 \times 10^{-2})(5 \times 10^{-2})(1.5 \times 10^{-3})]m^3 - [2(7.8 \times 10^{-7})]m^3$$

$$= 2.19 \times 10^{-6} m^3$$

Determination of the minimum number of cells to be seeded:

$$Number\ of\ cells = \frac{Volume\ of\ space}{[(area\ of\ skin\ cell)(thickness\ of\ structure)]} \quad (3.2)$$

$$= \frac{2.19 \times 10^{-6}}{[(25 \times 10^{-6})(1.5 \times 10^{-3})]}$$

$$= 58.4\ cell$$

Appendix B

Tables of Results for 3D printed Scaffold Tensile Test

Table A-1: *Tensile Test Results for 3D printed Scaffold Sample 1*

Display Name	Value	Unit	Original Value	Description
Modulus	239	MPa	0.239	The Young's modulus of the specimen.
Peak Load	0.034	kN	0.034	
Peak Stress	2	MPa	2	The maximum stress determined from the data.
Strain at Break	0.009	mm/mm	0.009	
Test Run End Reason	Break Detected		Break Detected	
Thickness	2	mm	2	The thickness of the specimen.
Width	10	mm	10	The width of the specimen.

Table A-2: *Tensile Test Results for 3D printed Scaffold Sample 2.*

Display Name	Value	Unit	Original Value	Description
Modulus	50	MPa	0.05	The Young's modulus of the specimen.
Peak Load	0.009	kN	0.009	
Peak Stress	0.4	MPa	0.4	The maximum stress determined from the data.
Strain at Break	0.021	mm/mm	0.021	
Test Run End Reason	Test Stopped		Test Stopped	
Thickness	2	mm	2	The thickness of the specimen.
Width	10	mm	10	The width of the specimen.

Table A-3*: Tensile Test Results for 3D printed Scaffold Sample 3.*

Display Name	Value	Unit	Original Value	Description
Modulus	86	MPa	0.086	The Young's modulus of the specimen.
Peak Load	0.035	kN	0.035	
Peak Stress	2	MPa	2	The maximum stress determined from the data.
Strain at Break	0.024	mm/mm	0.024	
Test Run End Reason	Break Detected		Break Detected	
Thickness	2	mm	2	The thickness of the specimen.
Width	10	mm	10	The width of the specimen.

***Table A-4**: Tensile Test Results for 3D printed Scaffold Sample 4.*

Display Name	Value	Unit	Original Value	Description
Modulus	194	MPa	0.194	The Young's modulus of the specimen.
Peak Load	0.054	kN	0.054	
Peak Stress	3	MPa	3	The maximum stress determined from the data.
Strain at Break	0.021	mm/mm	0.021	
Test Run End Reason	Test Stopped		Test Stopped	
Thickness	2	mm	2	The thickness of the specimen.
Width	10	mm	10	The width of the specimen.

***Table A-5**: Tensile Test Results for 3D printed Scaffold Sample 5.*

Display Name	Value	Unit	Original Value	Description
Modulus	111	MPa	0.111	The Young's modulus of the specimen.
Peak Load	0.031	kN	0.031	
Peak Stress	2	MPa	2	The maximum stress determined from the data.
Strain at Break	0.018	mm/mm	0.018	
Test Run End Reason	Break Detected		Break Detected	
Thickness	2	mm	2	The thickness of the specimen.
Width	10	mm	10	The width of the specimen.

Stress-Strain Graphs for Tensile Test 3D printed Scaffold Samples

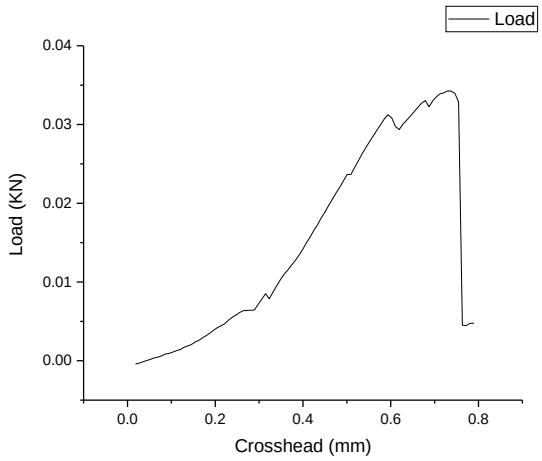

***Figure A- 1:** Tensile Test Stress-Strain Graph for 3D printed Scaffold Sample 1*

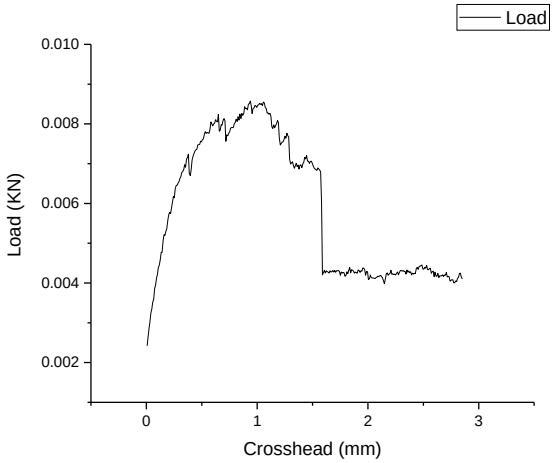

***Figure A- 2**: Tensile Test Stress-Strain Graph for 3D printed Scaffold Sample 2*

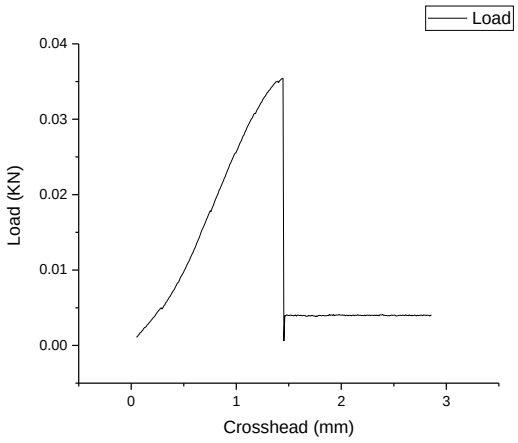

***Figure A- 3**: Tensile Test Stress-Strain Graph for 3D printed Scaffold Sample 3*

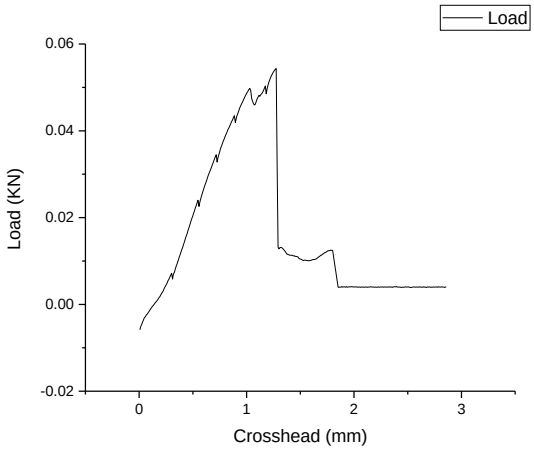

***Figure A- 4:** Tensile Test Stress-Strain Graph for 3D printed Scaffold Sample 4*

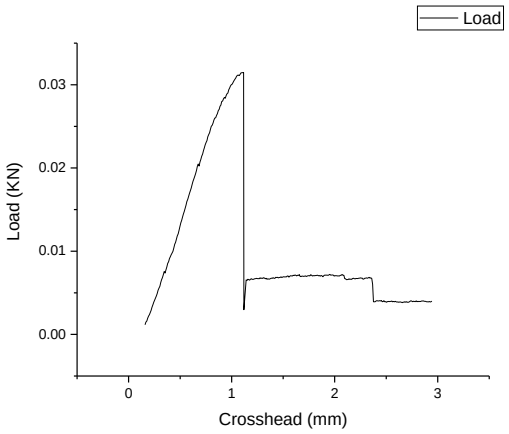

***Figure A- 5:** Tensile Test Stress-Strain Graph for 3D printed Scaffold Sample 5*

Tables of Results for 3D Casted Scaffold Tensile Test

***Table A- 6:** Tensile Test Results for 3D Casted (PLA) Scaffold Sample*

Display Name	Value	Unit	Original Value	Description
Peak Stress	0.2	kN/mm²	0.2	The maximum stress determined from the data.
Peak Load	5	kN	5	
Strain at Break	0.149	mm/mm	0.149	
Modulus	133.3	MPa	133.3	The Young's modulus of the specimen.
Width	10	mm	10	The specimen width.
Thickness	3	mm	3	The specimen thicknesses.

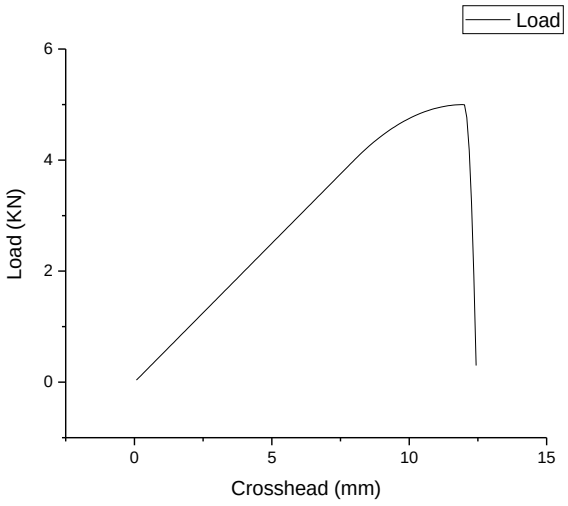

Figure A- 6: *Tensile Test Stress-Strain Graph for 3D Casted (PLA) Scaffold Sample*

Table A- 7: *Tensile Test Results for 3D Casted (PLA and PEG) Scaffold Sample*

Display Name	Value	Unit	Original Value	Description
Peak Stress	0.2	kN/mm²	0.2	The maximum stress determined from the data.
Peak Load	5	kN	5	
Strain at Break	0.149	mm/mm	0.149	
Modulus	133.3	MPa	133.3	The Young's modulus of the specimen.
Width	10	mm	10	The specimen width.
Thickness	3	mm	3	The specimen's thickness

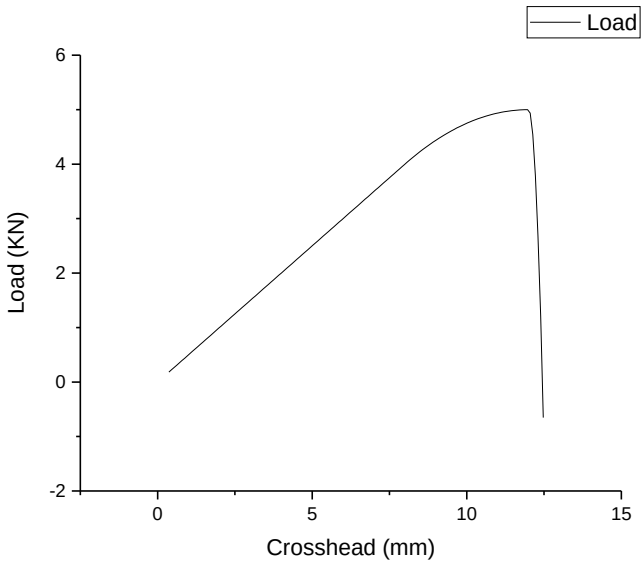

Figure A- 7*: Tensile Test Stress-Strain Graph for 3D Casted (PLA and PEG) Scaffold Sample*

Appendix C

Tables of Results for 3D printed Scaffold Stiffness Test

Table A- 8: *Bend Test Results for 3D printed Scaffold Sample 1.*

Display Name	Value	Unit	Original Value	Description
Peak Load	-0.00275	kN	-0.00275	
Peak Stress	-0.092	MPa	-0.1	The maximum stress determined from the data.
Flexural Modulus	0.375	MPa	0.375	
Width	20	mm	20	The specimen width.
Thickness	1.5	mm	1.5	The specimen's thickness.

Table A- 9: *Bend Test Results for 3D printed Scaffold Sample 2.*

Display Name	Value	Unit	Original Value	Description
Peak Load	-0.0032	kN	-0.0032	
Peak Stress	-0.107	MPa	-0.0667	The maximum stress determined from the data.
Flexural Modulus	0.5	MPa	0.5	
Width	20	mm	20	The specimen width.
Thickness	1.5	mm	1.5	The specimen's thickness.

Table A- 10: *Bend Test Results for 3D printed Scaffold Sample 3.*

Display Name	Value	Unit	Original Value	Description
Peak Load	-0.00125	kN	-0.00125	
Peak Stress	-0.0416	MPa	-0.0416	The maximum stress determined from the data.
Flexural Modulus	0.3	MPa	0.3	
Width	20	mm	20	The specimen width.
Thickness	1.5	mm	1.5	The specimen's thickness.

Table A- 11: *Bend Test Results for 3D printed Scaffold Sample 4.*

Display Name	Value	Unit	Original Value	Description
Peak Load	-0.00325	kN	-0.00325	
Peak Stress	-0.108	kN/mm²	-0.108	The maximum stress determined from the data.
Flexural Modulus	0.25	MPa	0.25	
Width	20	mm	20	The specimen width.
Thickness	1.5	mm	1.5	The specimen's thickness.

Table A- 12: *Bend Test Results for 3D printed Scaffold Sample 5.*

Display Name	Value	Unit	Original Value	Description
Peak Load	-0.00475	kN	-0.00475	
Peak Stress	-0.158	kN/mm²	0.158	The maximum stress determined from the data.
Flexural Modulus	0.33	MPa	0.33	
Width	20	mm	20	The specimen width.
Thickness	1.5	mm	1.5	The specimen's thickness.

Stress-Strain Graphs for Stiffness Test 3D printed Scaffold Samples

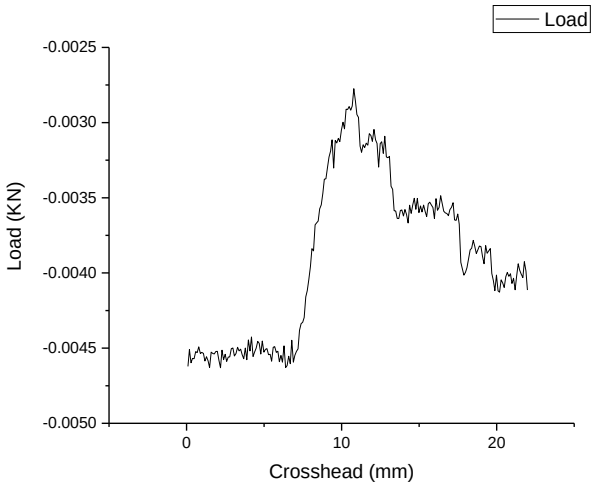

Figure A- 8: *Bend Test Stress-Strain Graph for 3D printed Scaffold Sample 1*

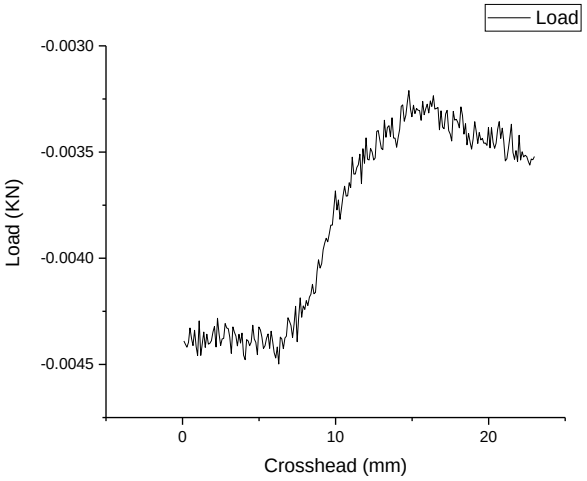

Figure A- 9: *Bend Test Stress-Strain Graph for 3D printed Scaffold Sample 2*

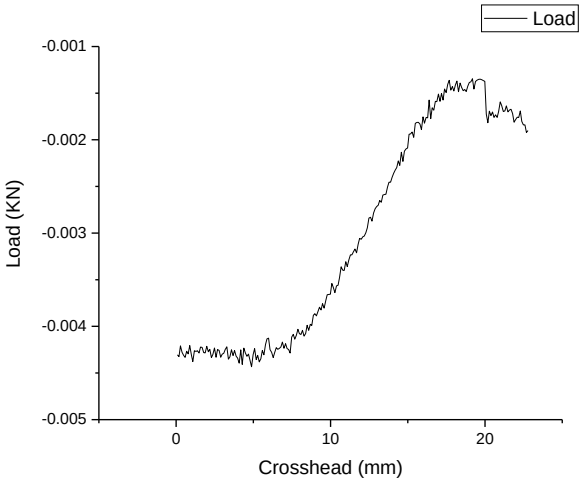

***Figure A- 10**: Bend Test Stress-Strain Graph for 3D printed Scaffold Sample 3*

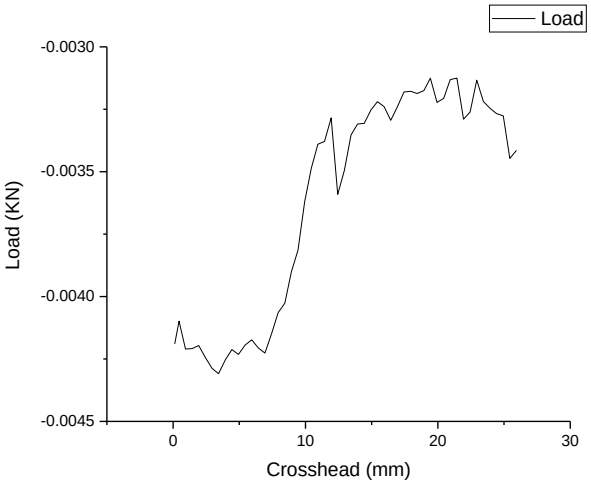

***Figure A- 11:** Bend Test Stress-Strain Graph for 3D printed Scaffold Sample 4*

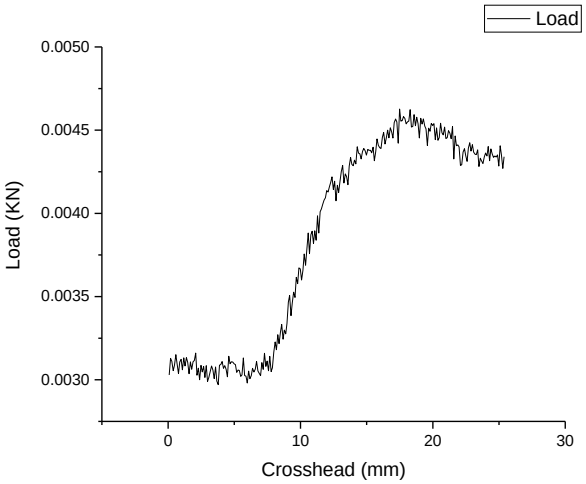

***Figure A- 12:** Bend Test Stress-Strain Graph for 3D printed Scaffold Sample 5*

Tables of Results for 3D Casted Scaffold Stiffness Test

Table A- 13: *Bend Test Results for 3D Casted (PLA) Scaffold Sample*

Display Name	Value	Unit	Original Value	Description
Peak Load	0.008	kN	11.082	
Peak Stress	0.267	MPa	0.267	The maximum stress determined from the data.
Flexural Modulus	0.67	MPa		
Width	10	mm	10	The specimen width.
Thickness	3	mm	3	The specimen's thickness.

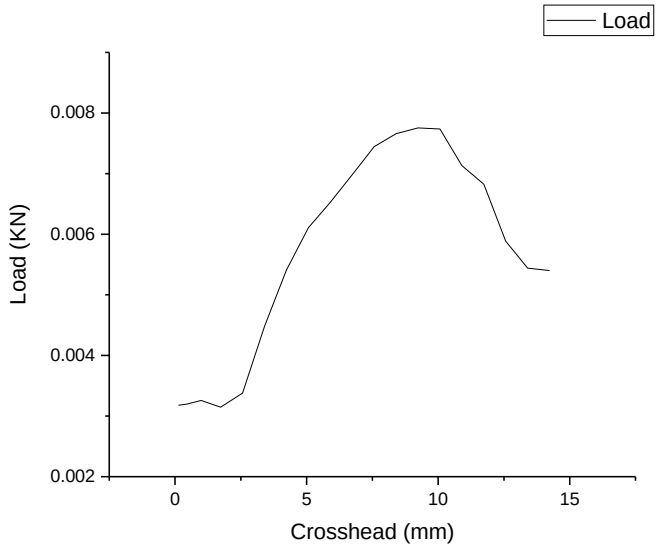

Figure A- 13: *Bend Test Stress-Strain Graph for 3D Casted (PLA) Scaffold Sample*

Table A- 14*: Tensile Test Results for 3D Casted (PLA and PEG) Scaffold Sample*

Display Name	Value	Unit	Original Value	Description
Peak Load	0.0071	kN	3.759	
Peak Stress	0.236	MPa	0.236	The maximum stress determined from the data.
Flexural Modulus	0.2	MPa	0.002	
Width	10	mm	10	The specimen width.
Thickness	3	mm	3	The specimen's thickness.

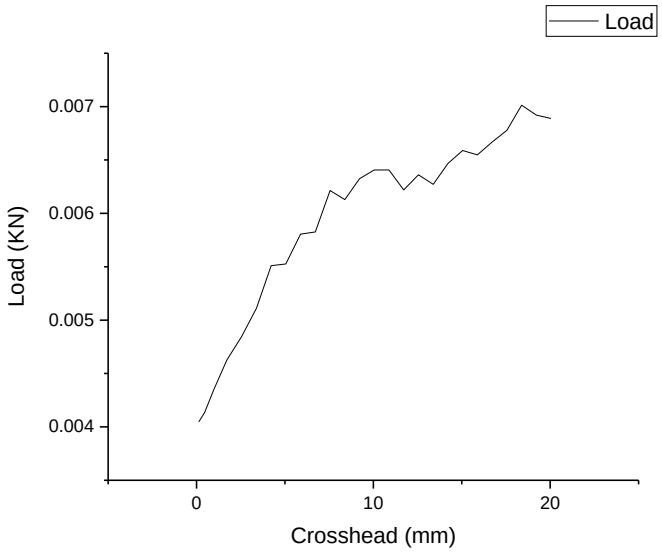

Figure A- 14: *Bend Test Stress-Strain Graph for 3D Casted (PLA and PEG) Scaffold Sample*